A Study on Yielding Function of Aluminum Honeycomb

Authors:

Shigeki Kojima
TOYOTA COMMUNICATION SYSTEMS CO., LTD. , Japan

Tsuyoshi Yasuki, Satoshi Mikutsu
Toyota Motor Corporation, Japan

Toshikazu Takatsudo
THE YOKOHAMA RUBBER CO., LTD. , Japan

Keywords:
Automotive Crashworthiness, Offset Deformable Barrier (ODB),
Aluminum Honeycomb, and Material-126

Abstract

This paper describes newly developed yielding function of aluminum honeycomb. Physical compression tests of aluminum honeycomb were performed and it was found that yielding stress of aluminum honeycomb highly depended up on direction of compression. Using these test data, a yielding function was newly derived as a function of volumetric change and angle of compression.

The yielding function was introduced to MAT126 as an option. ODB frontal collision analysis result with the yielding function showed much better correlation with test results than with MAT126 without the option.

1. Introduction

In using offset frontal collision analysis to predict the amount of vehicle deformation, it is essential for the ODB model (Offset Deformable Barrier model) to replicate the compression property of aluminum honeycomb accurately. Numerous studies have been published of the compression property of aluminum honeycomb along a single axis, but in an offset frontal collision, the aluminum honeycomb is compressed not just along one axis, but also in the oblique direction.

This paper focuses on the compression property of aluminum honeycomb in the oblique direction. Independently conducted tests of aluminum honeycomb compression indicated that the yielding function of aluminum honeycomb is dependent on the direction of compression. The yielding function that was derived was incorporated into the material model for LS-DYNA in an attempt to improvement accuracy of vehicle deformation prediction, and an offset frontal collision analysis was carried out.

2. Motivation of Study

2.1 Comparison of test results and FEM analysis for full overlap frontal collision

The first stage in the FEM analysis was to verify the computational accuracy of the vehicle model by analyzing a full overlap frontal collision using a rigid barrier and the vehicle model. Figure 1 shows the deformed shape of the vehicle after the collision, while Figure 2 tracks the history of the force acting on the barrier.

Both the test results and the FEM analysis show that front side member is bent vertically in the height direction after the collision, and the deformation modes generally match. Also, the barrier force history from the FEM analysis generally matches the test results, replicating particularly well the process from the start of the collision until the maximum barrier force is reached. It can therefore be said that this vehicle model is sufficiently accurate for comparison with the test results.

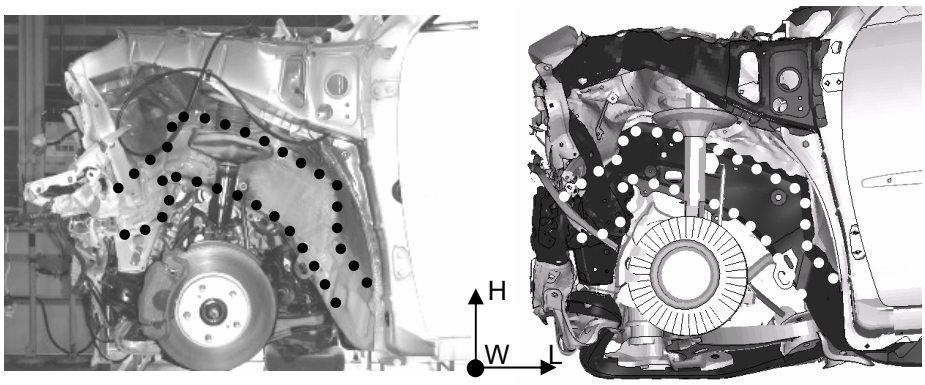

Fig. 1 Deformed shape of vehicle after a full overlap frontal collision

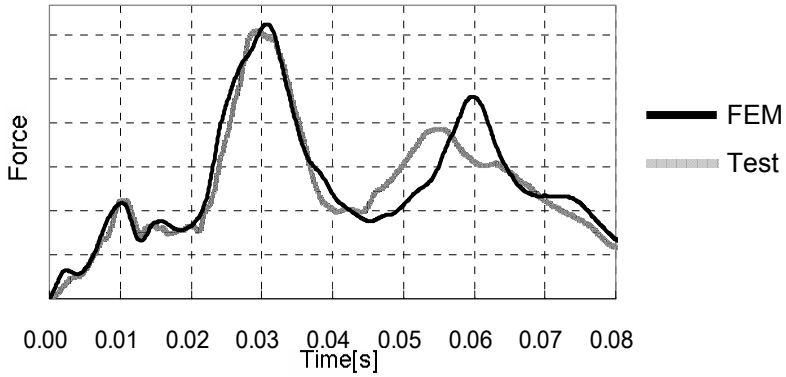

Fig. 2 Time history of barrier force

2.2 Comparison of test results and FEM analysis for offset frontal collision

An analysis was carried out of an offset frontal collision using the vehicle model described above and an ODB model. Figure 3 shows the deformed shape of the vehicle after the collision. Note that in the ODB model, MAT126 was used as the material model for the aluminum honeycomb.

The test results show that the front side member is bent vertically in the height direction after the collision, but the FEM analysis shows it bent horizontally in the width direction. Thus a difference is observed between the test results and the FEM analysis in the deformation modes for the front side member.

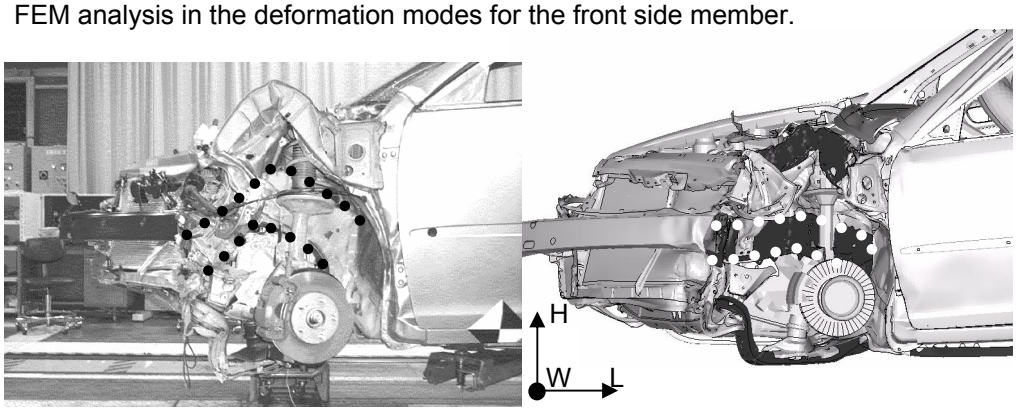

Fig. 3 Deformed shape of vehicle after ODB frontal collision

3. Assumption

An attempt was made to identify the reason why the bending mode of the front side member is different in the offset frontal collision test and the FEM analysis. Figure 4 shows the deformed shapes of the ODB and the vehicle in the FEM analysis at 30 milliseconds after impact, when the front side member buckles.

There is little deformation in region B of the core honeycomb, which is located on the outer side of the front side member, strongly suggesting that the compressive strength is too great. It is surmised that the force generated by the deformation of region B is transmitted through the obliquely inclined bumper honeycomb to exert excessive pressure on the front side member in the width direction, so that it bends horizontally.

An examination of the deformation mode of the core honeycomb shows that region A is compressed in the length direction, while region B is compressed obliquely to the length direction. It is therefore assumed that the horizontal bending of the front side member in the FEM analysis is caused by the excessive compressive strength of region B, which is to say, the excessive compressive strength of the aluminum honeycomb model in relation to deformation in the oblique direction.

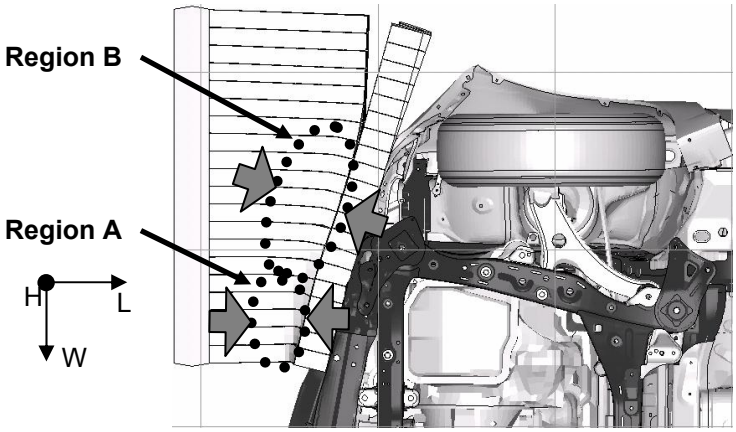

Fig. 4 Deformed shape of ODB and vehicle [t=30ms]

4. Yielding Function

In order to verify the assumption, the compressive strength of aluminum honeycomb was studied to see if it varied according to direction. First, test pieces measuring 150 x 150 x 50 millimeters were cut out of the barrier's core honeycomb at intervals of 10 degrees in relation to the width direction and subjected to static compression tests. Figure 5 illustrates the concept of the test, while Figure 6 shows the relationship between the compression stroke and stress. Here, stress is calculated as the compressive load divided by the initial cross sectional area of the test piece (150x150 mm^2). When the test piece is compressed 10 millimeters or more, the stress is nearly the same in both test pieces.

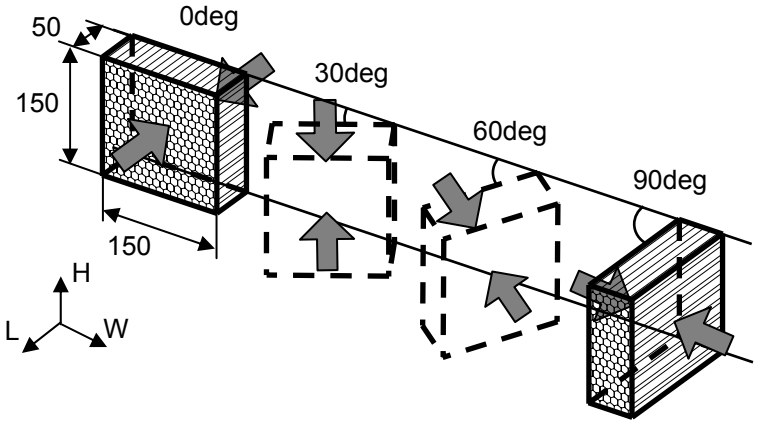

Fig. 5 Concept of aluminum honeycomb compression test

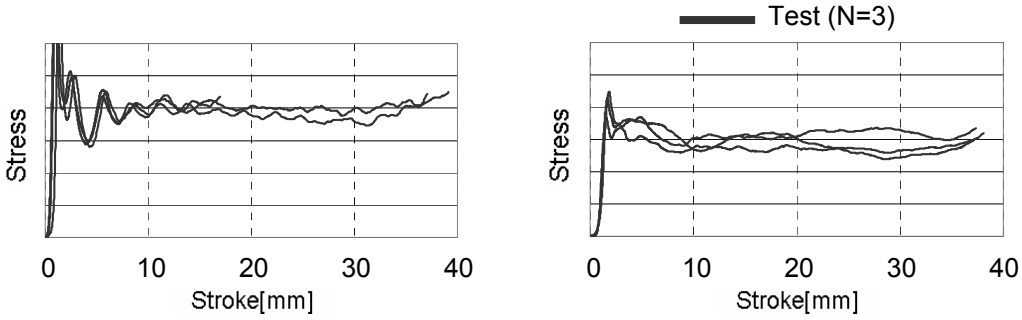

(a) Zero-degree test piece (b) 30-degree test piece

Fig. 6 Relationship of compression stroke and stress

An FEM analysis that simulates the compression test was carried out using the same aluminum honeycomb model that was used for the ODB model. Figure 7 shows the relationship between compressive stress and the angle at which the test piece was cut when the stroke is 10 millimeters, in both the compression test and the FEM analysis.

In the tests, the compressive stress in the zero-degree test piece was the highest value measured, and as the angle at which a given test piece was cut increases, the compressive stress decreases. Particularly in test pieces cut at angles of 60 degrees or more, the compressive stress drops dramatically, to one-tenth or less than that of the zero-degree test piece. By contrast, in the aluminum honeycomb model (MAT126) that was used for the ODB model, the compressive stress is highest in the test piece that is cut at an angle of 30 degrees. When the model is compared to the test results, it is clear that the compressive stress is too great in all the oblique direction regions, i.e., at all angles other than zero and 90 degrees. In other words, there is a significant discrepancy between the aluminum honeycomb model (MAT126) used for the ODB model and the actual honeycomb used in the tests.

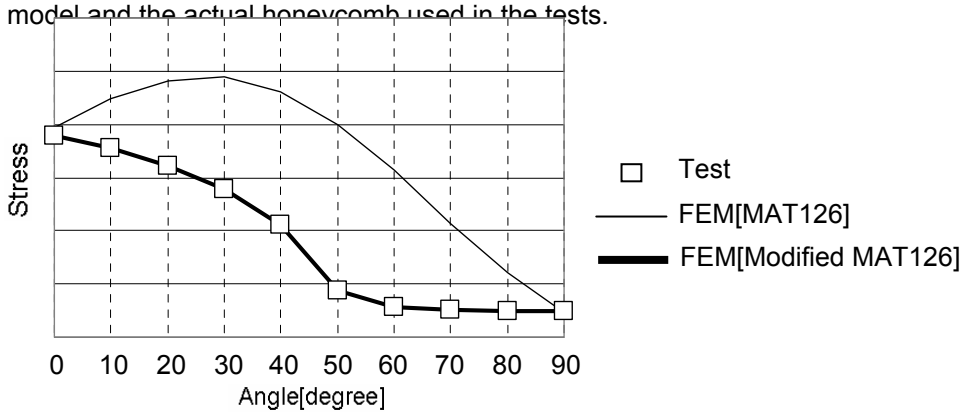

Fig. 7 Relationship between test piece cutting angle and compressive stress

In order to replicate the variation in compressive strength of the actual aluminum honeycomb according to direction, the yielding function shown as Equation 1 below was incorporated into the material model MAT126 with the cooperation of Livermore Software Technology Corporation (LSTC). The thick line in Figure 7 shows the relationship between the test piece cutting angle and compressive stress in an FEM analysis that uses the modified MAT126. In the modified MAT126, the degree to which compressive strength varies with direction can be freely defined, so the relationship it shows between the test piece cutting angle and compressive stress matches the test results. Thus, the variation in compressive strength according to direction that is exhibited by the actual

aluminum honeycomb is replicated by applying the yielding function shown in Equation 1.

$$\sigma^{y}(\varphi,\varepsilon^{vol}) = \sigma^{b}(\varphi) + (\cos\varphi)^2\sigma^{s}(\varepsilon^{vol}) + (\sin\varphi)^2\sigma^{w}(\varepsilon^{vol}) \quad (1)$$

φ = angle with the strong axis

$\sigma^{b}(\varphi)$ = yield stress as a tabulated function of φ

$\sigma^{s/w}(\varepsilon^{vol})$ = stiffening as a tabulated function of ε^{vol}

5. Results

5.1 Comparison of test results and FEM analysis for barrier inspection

An ODB model was created that uses the modified MAT126 to replicate accurately the compressive strength of aluminum honeycomb from the oblique direction. A barrier-inspection FEM analysis was then carried out to verify the computational accuracy of the ODB model that uses the modified MAT126. The inspection was carried out by causing two types of impactors to collide with the ODB at an initial velocity. The impactors are different sizes and are made specifically for inspection.

Figure 8(a) illustrates the concept of the barrier-inspection FEM analysis using a Type A impactor, while Figure 8(b) shows the relationship between the impactor stroke and the barrier force. In the ODB model that uses the modified MAT126, the barrier force approximates the test results when the stroke is 450 millimeters or longer.

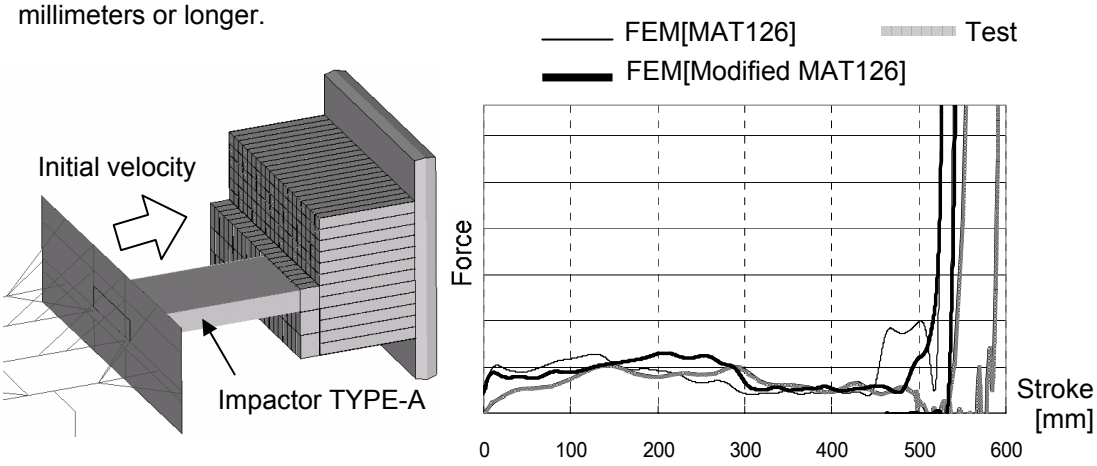

(a)Impactor TYPE-A test FE model (b)Comparison of Force-Stroke Curves

Fig. 8 Impactor TYPE-A test

Figure 9(a) illustrates the concept of the barrier-inspection FEM analysis using a Type B impactor, and Figure 9(b) shows the relationship between the impactor stroke and the barrier force. In the ODB model that uses the modified MAT126, the barrier force approximates the test results when the stroke is 250 millimeters or longer. It can therefore be said that in the barrier-inspection FEM analysis, the ODB model that uses the modified MAT126 demonstrates sufficient computational accuracy.

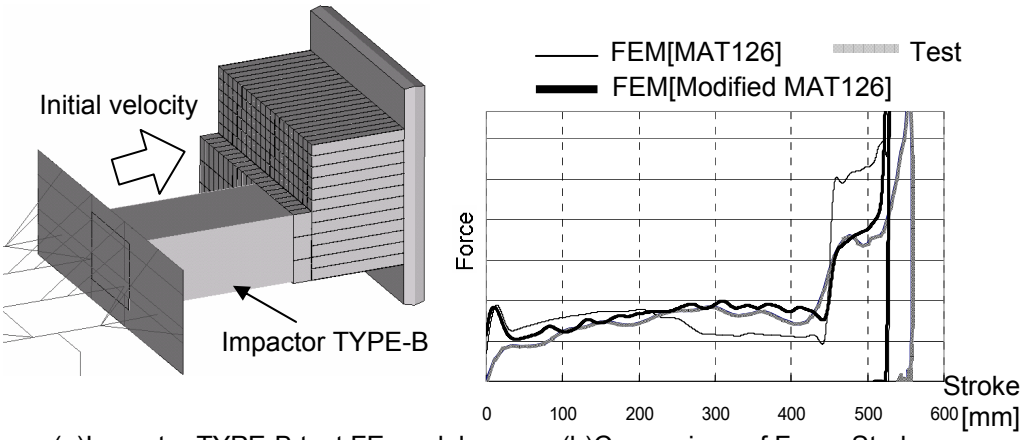

(a)Impactor TYPE-B test FE model (b)Comparison of Force-Stroke Curves

Fig. 9 Impactor TYPE-B test

5.2 Comparison of test results and FEM analysis for offset frontal collision

An analysis of an offset frontal collision was carried out using the vehicle model described earlier and the ODB model that uses the modified MAT126. Figure 10 shows the deformed shape of the vehicle after the collision, and Figure 11 shows the barrier force history.

Looking at the FEM analysis for the front side member after the collision, vertical bending is seen in the height direction, and the deformation mode generally matches that of the test. The barrier force history from the FEM analysis also approximates the test results, showing a lower barrier force at 80 milliseconds after impact than was exhibited before MAT126 was modified. Thus, the ODB model that uses the modified MAT126 improves the prediction accuracy for both vehicle deformation and barrier force history in an offset frontal collision.

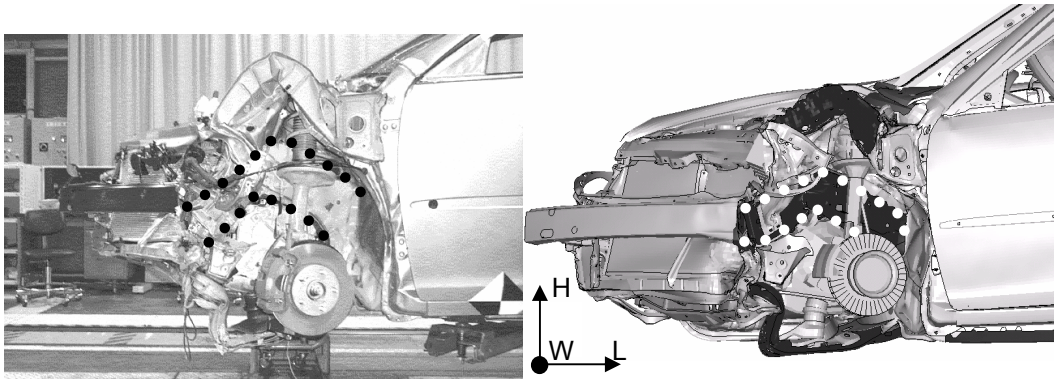

Fig. 10 Deformed shape of vehicle after ODB frontal collision

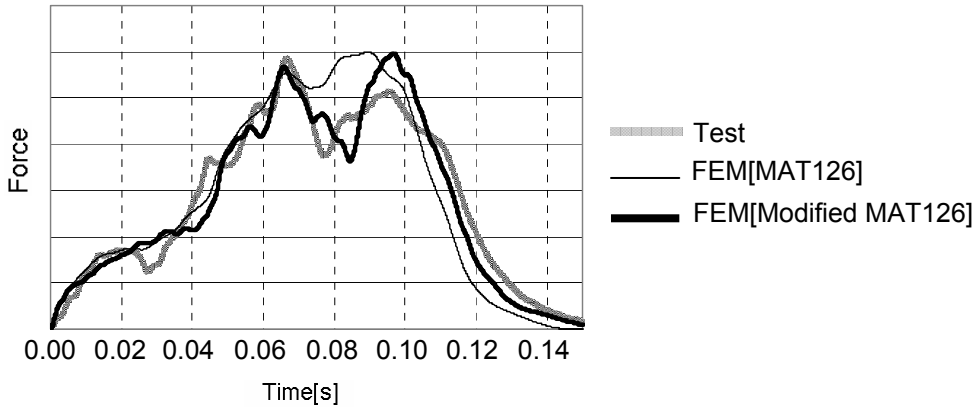

Fig. 11 Time history of barrier force

6. Discussion

In an attempt to identify the reason why the vertical bending of the front side member could be successfully replicated, the results of offset frontal collision analyses done before and after MAT126 was modified were compared. Figure 12 shows the deformed shapes of the ODB and the vehicle in the FEM analysis at 30 milliseconds after impact, when the front side member buckles.

In the ODB model that uses the modified MAT126 [Fig.12 (b)], the amount of deformation in the core honeycomb in the area around the front side member is greater than in the model using the older version of MAT126 [Fig. 12 (a)]. Also, as the amount of deformation in the core honeycomb increases, bending starts to occur in the bumper honeycomb. It is surmised that replicating both the compressive strength of the core honeycomb in the area around the front side member and the bending of the bumper honeycomb has the effect of reducing the excessive force on the front side member in the width direction, thereby allowing the vertical bending of the front side member to be replicated.

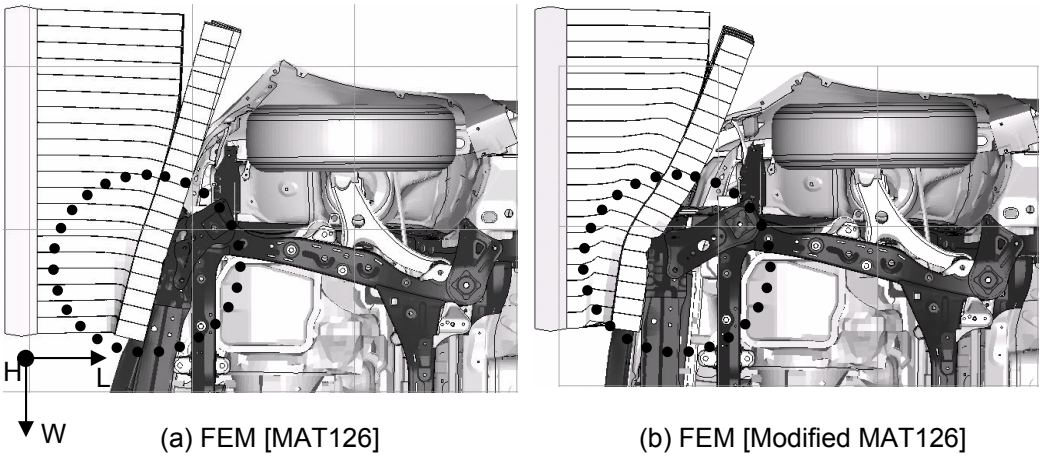

(a) FEM [MAT126] (b) FEM [Modified MAT126]

Fig. 12 Deformed shape of ODB and vehicle [t=30ms, Bottom view]

Figure 13 shows two cross section views of the front side member at 30 milliseconds after impact. It can be seen that in the ODB model that uses the modified MAT126 [Fig. 13 (b)], the amount of deformation in the front side member is less than in the model that uses the older version of MAT126 [Fig. 13 (a)], and the deformed shape of the vehicle is also significantly different.

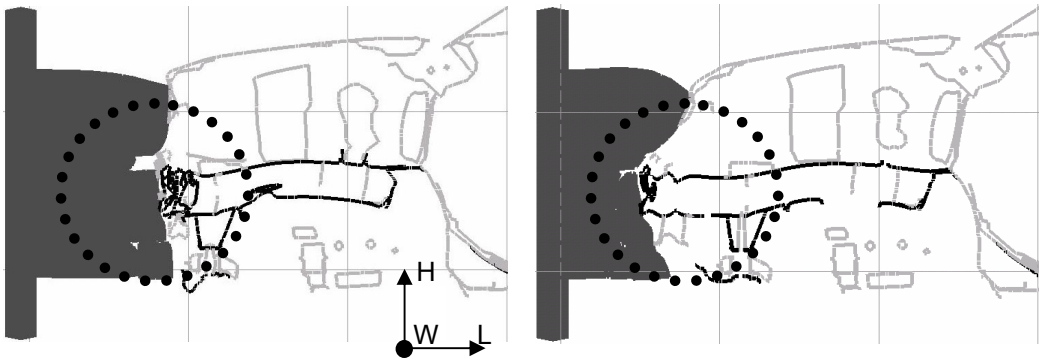

(a) FEM [MAT126] (b) FEM [Modified MAT126]

Fig. 13 Deformed shape of ODB and vehicle [t=30ms, Side view]

An attempt was also made to identify the reasons for the improvement in the barrier force history. Figure 14 shows the behavior of the engine and the gearbox at 80 milliseconds after impact, when the barrier force history produced by the ODB model that uses the modified MAT126 closely approximates the actual test results.

Before MAT126 was modified [Fig. 14 (a)], the engine and gearbox interfered with one another, but after MAT126 was modified [Fig. 14 (b)], the amount of engine rotation around the height axis increased and the amount of gearbox displacement in the width direction decreased, so that the engine and gearbox no longer interfere with one another. It is surmised that replicating the behavior of the engine and gearbox to avoid interference made it possible for the barrier force history to match the test results at around 80 milliseconds after impact.

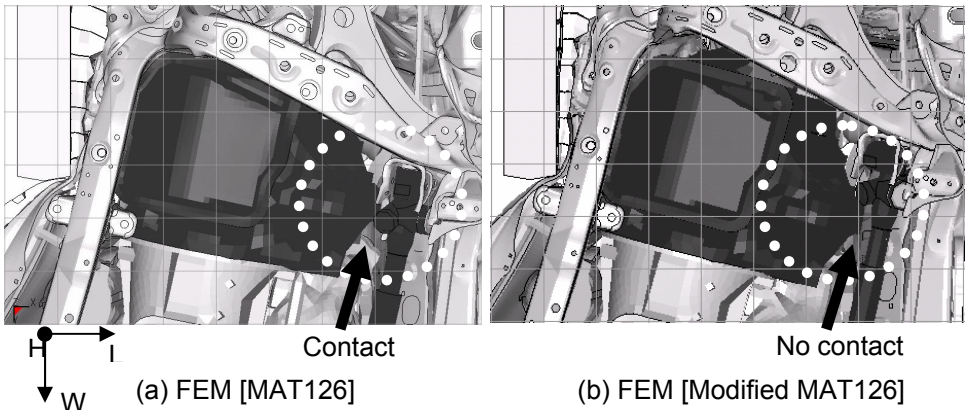

(a) FEM [MAT126] (b) FEM [Modified MAT126]

Fig. 14 Engine and gearbox behavior [t=80ms, Bottom view]

7. Conclusion

The dependency of the aluminum honeycomb yielding function on the direction of compression was clarified by means of compression tests on aluminum honeycomb. The yielding function thus derived was incorporated into the material model MAT126, an analysis of an offset frontal collision was carried out, and a significant improvement in the prediction accuracy for vehicle deformation and barrier force history was confirmed.

8. Acknowledgement

The authors wish to thank Livermore Software Technology Corporation for its cooperation in incorporating the yielding function into the material model MAT126.

References

1. Andreas Hirth, Paul Du Bois, Dr. Klaus Weimar, “A Material Model for Transversely Anisotropic Crushable Foams in LS-DYNA”, 7th International LS-DYNA Users Conference
2. Tsuyoshi Yasuki, Noriko Watanabe, “Vehicle Crash Analysis Applications to a Vehicle Development”, TOYOTA Technical Review Vol.51 No.1 Jun.2001
3. Koji Nojima, “Modeling and Accuracy of Offset Crash Deformable Barrier - Real phenomena and modeling technique –“, JSAE 2001
4. Moisey B Shkolnikov, “Honeycomb Modeling for Side Impact Moving Deformable Barrier(MDB)”, 7th International LS-DYNA Users Conference
5. Abdullatif K. Zaouk and Dhafer Marzougui, “Development and Validation of a US Side Impact Moveable Deformable Barrier FE Model”, 3rd European LS-DYNA Users Conference
6. Paul Du Bois, “Crashworthiness Engineering Course Notes”
7. J. Hallquist, “LS-DYNA Keyword Users Manual(Update), Version970/Rev5434”
8. J. Hallquist, “LS-DYNA Keyword Users Manual, Version970”
9. J. Hallquist, “LS-DYNA Theoretical Manual”